ISSN (Print) 1226-1750
ISSN (Online) 2233-6656
Journal of Magnetics 18(2), 168-172 (2013) http://dx.doi.org/10.4283/JMAG.2013.18.2.168

Development of High-Field ESR System Using SQUID Magnetometer and its Application to Measurement under High Pressure

T. Sakurai[1]*, K. Fujimoto[2], S. Okubo[3], H. Ohta[3], and Y. Uwatoko[4]

[1]*Center for Supports to Research and Education Activities, Kobe University, Kobe 657-8501, Japan*
[2]*Graduate School of Science, Kobe University, Kobe 657-8501, Japan*
[3]*Molecular Photoscience Research Center, Kobe University, Kobe 657-8501, Japan*
[4]*Institute for Solid State Physics, University of Tokyo, Kashiwa 277-8581, Japan*

(Received 31 May 2012, Received in final form 24 July 2012, Accepted 24 July 2012)

We have developed a high-field and high-frequency ESR system using a commercially available magnetometer equipped with the superconducting quantum interference device (SQUID). This is magnetization detection type ESR and ESR is observed as a change of the magnetization at the resonance condition under irradiation of the electromagnetic wave. The frequency range is from 70 to 315 GHz and the maximum magnetic field is 5 T. The sensitivity is estimated to be 10^{13} spins/G. The advantage of this system is that the high-field ESR measurements can be made very easily and quantitatively. Moreover, this high-field ESR can be applied to the measurements under pressure by using a widely used piston-cylinder pressure cell.

Keywords : ESR, high field, magnetization detection, SQUID, pressure cell

1. Introduction

High-field and high-frequency ESR measurement is one of the major trends in the ESR spectroscopy recently, because it has several advantages as compared with conventional X-band (~10 GHz) ESR system [1-7]. The advantages are high resolution of the *g*-value, observation of a broad line, observation of resonance with a large zero-field splitting, and so on. However, it is not always easy and convenience to operate such high-field ESR system for all researchers who desire high-field ESR spectra. In this study, we have developed a high-field and high-frequency ESR system which can be used very easily. The system uses a commercially available magnetometer equipped with the superconducting quantum interference device (SQUID). ESR is detected as a change of the magnetization at the resonance condition under the irradiation of the electromagnetic wave. Such magnetization detection type ESR using a commercial SQUID magnetometer was reported by Cage *et al*. first [8], and we have improved the sensitivity [9]. The most characteristic feature of this ESR measurement is that ESR measurement can be made quantitatively and very easily. Moreover, the system can be applied to the high pressure ESR measurement without difficulty by using a piston cylinder pressure cell. This is another advantageous point as compared with other ESR systems because the high-pressure ESR usually needs specialized equipments [10-18]. In this paper, we show the outline of the system and its application example. And, we also show the high-pressure ESR measurement by this system. These results demonstrate clearly that this ESR system provides a very useful technique to observe spin system microscopically even under the pressure.

2. Outline of System and Application Example

The principle of the magnetization detection type ESR using SQUID magnetometer is as follows. When the magnetic field H is swept under the irradiation of the electromagnetic wave with the frequency ν and the resonance condition $h\nu = g\mu_B H$ is satisfied, the resonance occurs, where h is the Planck constant, g is the g factor and μ_B is the Bohr magneton. The spins are excited and the transition occurs under the constraint of the selection

*Corresponding author: Tel: +81-78-803-5996
Fax: +81-78-803-5996, e-mail: tsakurai@kobe-u.ac.jp

This paper was presented at the ICM2012, Busan, Korea, July 8-13, 2012.

rule $|\Delta S_z| = 1$, for instance, from the $S_z = -1/2$ state to the $S_z = 1/2$ state for the $S = 1/2$ system. This implies that the magnetization also changes because the magnetization M is given by $M = M_0(n_{-1/2} - n_{1/2})$ for the $S = 1/2$ system, where $M_0 = Ng\mu_B$, N is the total spin number, and $n_{-1/2}$ and $n_{1/2}$ are the populations for the levels of $S_z = -1/2$ and $S_z = 1/2$, respectively. If the spins $N\Delta n$ are excited from the $S_z = -1/2$ to the $S_z = 1/2$ at the resonance condition, the magnetic moment decreases by $\Delta M = 2M_0\Delta n$. If such magnetization change ΔM can be detected, we can observe the ESR signal. The magnetization detection type ESR using SQUID magnetometer is the system which observes such magnetization change ΔM by the SQUID magnetometer, which is abbreviated as SQUID-ESR hereafter. Figure 1 shows the schematic diagram of the high-field and high-frequency SQUID-ESR system using a commercial SQUID magnetometer. MPMS (Quantum Design, Inc.) is used as the SQUID magnetometer. The maximum magnetic field is 5 T. The sample rod also works as a light pipe. The sample is set in a straw as usual and it is attached to the end of the light pipe. This sample rod was made of stainless and its inner and outer diameters are 5.4 and 6.0 mm, respectively. In the Cage's system the light pipe with smaller diameter (inner and outer diameters are 2.54 mm and 3.175 mm, respectively) was used [8]. On the other hand, we found that the sensitivity improves by increasing the diameter of the light pipe because the loss of the electromagnetic wave power due to reflection in the inside of the light pipe is suppressed [9]. The minimum detectable spin number was estimated as 10^{13} spins/G at 105 GHz (output power 52.5 mW) and 1.8 K for the above mentioned 6.0 mm light pipe while it was 10^{14} spins/G for the light pipe with almost the same diameter with that used in the Cage's system. The improvement of the sensitivity by about one order has been achieved in this study. Although the sensitivity of 10^{13} spins/G is not necessarily high as compared with the X-band ESR system (typically its sensitivity is about 10^{10} spins/G), the SQUID-ESR has several advantages as mentioned later. Gunn oscillators are used as electromagnetic wave sources and they are set at the top of the light pipe. We confirmed that the ESR measurements can be performed in the frequency range from 70 to 315 GHz by changing the Gunn oscillator [9]. It should be noted that the operation of MPMS for the SQUID-ESR measurement is the same with that for usual magnetization measurement.

Figure 2 shows typical SQUID-ESR spectra obtained by this system. A well-known organic radical compound 2, 2-diphenyl-1-picrylhydrazyl (DPPH) was used as a sample. The dotted line is the magnetization curve of DPPH and it is obtained by usual magnetization measurement. On the other hand, the solid lines are obtained under irradiation of the electromagnetic wave. The sharp decreases were observed and these decreases are due to the spin excitation at the resonance condition as is mentioned above. The intensity of the ESR signal depends on the output power of the Gunn oscillator mainly. Thus, the ESR signals were observed very clearly by this SQUID-ESR system.

The total spin number of DPPH obtained from its mass is usually overestimated because of deactivation of radicals in the sample. However, the accurate number N can be estimated in this measurement by fitting the Brillouin

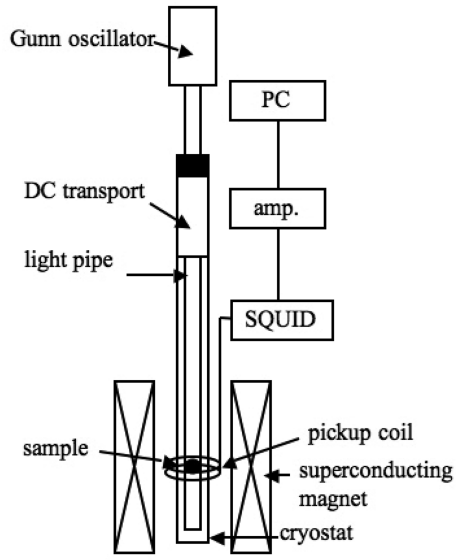

Fig. 1. Schematic diagram of high-field and high-frequency SQUID-ESR system.

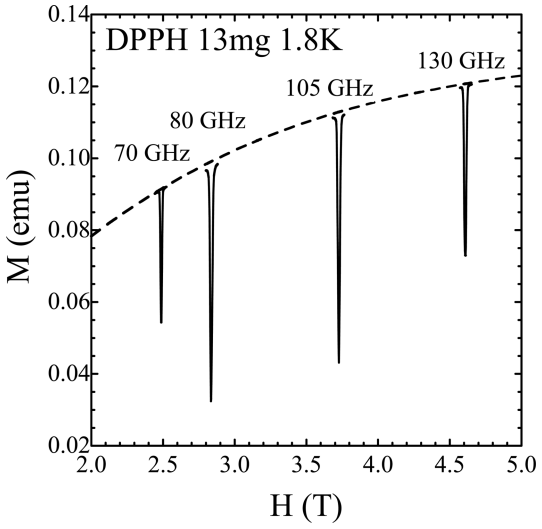

Fig. 2. SQUID-ESR spectra for DPPH at 1.8 K obtained at various frequencies.

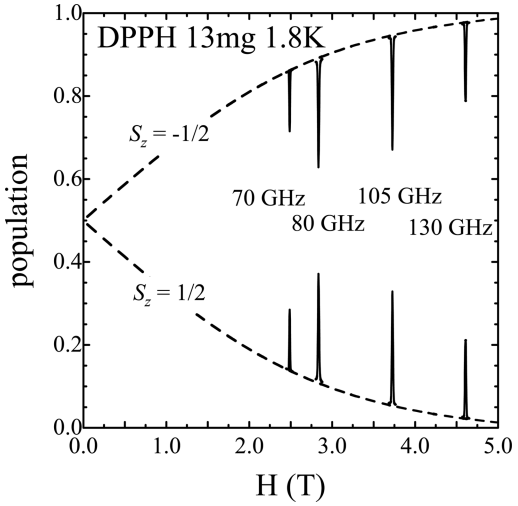

Fig. 3. Magnetic field dependence of the populations of S_z = −1/2 and S_z = 1/2 levels for DPPH at 1.8 K (dotted lines). The solid lines show the change of the population at the resonance condition.

function $M = M_0\tanh(g\mu_B H/k_B T)$ to the magnetization curve with directly obtained g-value from the resonance field. From this fitting we obtained spin number N accurately and about 70% of radicals were found to remain active. We can also calculate the populations $n_{-1/2}$ and $n_{1/2}$ by using this spin number N and the relation $M = M_0(n_{-1/2} - n_{1/2})$ as shown in Fig. 3. At the corresponding field to the frequency of 80 GHz (~2.8 T), for instance, the S_z = −1/2 and the S_z = 1/2 levels are occupied by about 90% and 10%, respectively, when the electromagnetic wave is not irradiated as shown by the dotted lines in Fig. 3. On the other hand, the population of the S_z = −1/2 level decreases to about 60% and that of the S_z = 1/2 level increases to about 40% due to the ESR transition under the irradiation of the electromagnetic wave as shown by the solid lines in Fig. 3. These analyses demonstrate that the ESR measurement can be made quantitatively by this SQUID-ESR system and this is advantage as compared with other conventional ESR measurements.

3. Application to high-pressure measurement

Next we show the application of this SQUID-ESR system to the high-pressure ESR measurement. The pressure is one of the most important parameters in the solid state physics because it changes the interactions between the electron spins continuously and it sometimes leads to novel physical phenomena [19-22]. Although high-pressure ESR is a powerful means to observe the spin system subjected to the pressure microscopically, it usually needs

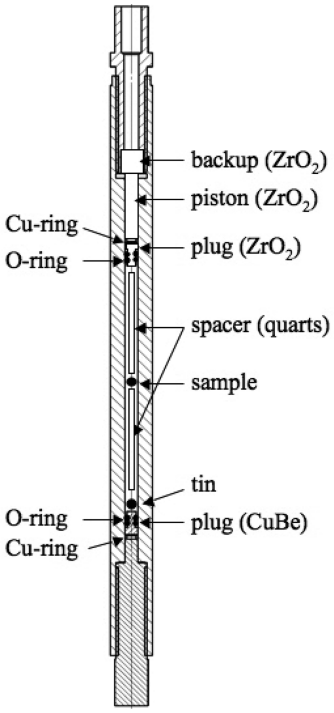

Fig. 4. Cross section of the piston cylinder pressure cell for high pressure SQUID-ESR measurement.

specialized equipments [10-18]. On the contrary, the SQUID-ESR can be applied to the high-pressure ESR very easily. For the high-pressure ESR measurement, the combination of the SQUID-ESR system and the piston-cylinder pressure cell as shown in Fig. 4 is used. The pressure cell shown in Fig. 4, which was originally developed by Uwatoko *et al*. [23], is very widely used for the magnetization measurement and it is recently commercially available. The cylinder and clamping bolts are all made of non-magnetic CuBe alloy. In order to introduce the electromagnetic wave into the sample space, the upper inner parts made of CuBe alloy were replaced by those made of ZrO_2 which was already known to have relatively good transmittance of electromagnetic wave [24] as shown in Fig. 4. This pressure cell is connected to the end of light pipe. Figure 5 is typical high-pressure SQUID-ESR spectra by this system. The sample is an S = 1 paramagnet $NiSnCl_6{\cdot}6H_2O$ whose magnetic ion is Ni^{2+}. Due to the crystal field surrounding this magnetic ion, the energy splitting occurs at zero field, which is called as the zero-field splitting and characterized by the D-value, between the S_z = 0 state and the S_z = ±1 states and this causes the signal splitting as shown in the inset of Fig. 6. We already found that the D-value increases as the pressure is increased for this material [24]. The dotted and solid lines in Fig. 5 were obtained when the electromagnetic wave was not irradiated and irradiated, respectively. There are two

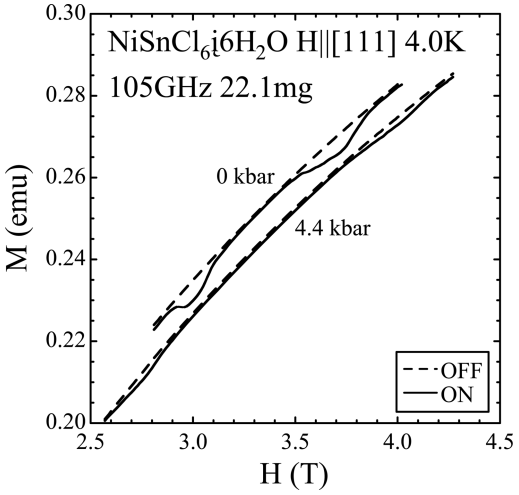

Fig. 5. Magnetization curves of $NiSnCl_6{\cdot}6H_2O$ at 0 kbar and 4.4 kbar with or without the irradiation of electromagnetic wave.

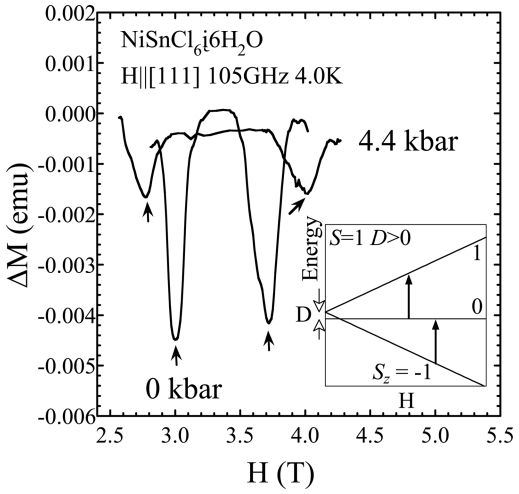

Fig. 6. SQUID-ESR spectra at 0 kbar and 4.4 kbar. The inset shows the schematic energy-field diagram of this material.

discrepancies between the dotted and solid lines at around 3.0 and 3.7 T obviously at 0 kbar and these two discrepancies are also seen at around 2.8 and 4.1 T at 4.4 kbar. In order to see these changes clearly we subtract the magnetization data obtained without irradiation from that obtained with irradiation as shown in Fig. 6. It shows clearly that the two signals are observed and the splitting width of these two signals becomes larger at 4.4 kbar. This is concluded to be due to the increase of the *D*-value by applying the pressure. It should be noticed that the magnetization was suppressed under pressure as shown by the dotted lines in Fig. 4. It is caused by the increase of the *D*-value under pressure and this fact is consistent with the ESR measurements. Thus, the high-pressure SQUID-ESR measurements have been performed by the combination of the SQUID-ESR system and the widely used piston-cylinder pressure cell, which was modified so that the electromagnetic wave can be introduced. Another important point is that the well-established pressure calibration method was used in this system. The change of the superconducting transition temperature of tin under pressure, which is one of the most reliable pressure calibration methods, can be applied in this system. As shown in Fig. 4 tin is also set in the sample space of the pressure cell and the superconducting transition temperature of tin is determined from its temperature dependence of the magnetic moment. The high-pressure SQUID-ESR measurement and the pressure calibration can be continuously done and it is very convenient. The pressure of 4.4 kbar in this experiment was obtained by this calibration method. Recently, we have developed a new pressure cell for the SQUID-ESR measurement. We have achieved the maximum pressure of 15 kbar by this new cell and the sensitivity has been also improved. Its detailed description will appear elsewhere [25].

4. Summary

We have developed a high-field and high-frequency ESR system using commercially available SQUID magnetometer. The maximum magnetic field is 5 T and the frequency range is from 70 to 315 GHz. We have improved the sensitivity and it was estimated as 10^{13} spins/G at 105 GHz and 1.8 K. The system was found to provide us a very useful high-field ESR technique by which ESR measurement can be done quantitatively and very easily. Moreover, we confirmed that this ESR technique can be applied to the high pressure ESR measurement by using the widely used piston cylinder pressure cell. One of the characteristic features of this high-pressure SQUID-ESR system is that the well-established pressure calibration method can be used in addition to the easy handling.

Acknowledgment

This research was partially supported by Grant-in-Aid for Scientific Research (C) (No. 22540349) and Creative Scientific Research (No. 19GS1209) from Japan Society for the Promotion of Science.

References

[1] M. Motokawa, H. Ohta, and N. Maki, Int. J. Infrared & Millimeter Waves **12**, 149 (1991).
[2] S. S. Eaton and G. R. Eaton, in C. P. Poole Jr. and H. A.

Farach Eds., Handbook of electron spin resonance, vol. 2, Springer, New York (1999).
[3] A. K. Hassan, L. A. Pardi, J. Krzystek, A. Sienkiewicz, P. Goy, M. Rohrer, and L.-C. Brunel, J. Magn. Reson. **142**, 300 (2000).
[4] L. C. Brunel, A. Caneschi, A. Dei, D. Frishelli, D. Gatteschi, A. K. Hassan, L. Lenci, M. Martinelli, C. A. Massa, L. A. Pardi, F. Popescu, I. Ricci, and L. Sorace, Res. Chem. Intermed. **28**, 215 (2002).
[5] H. Ohta, H. Nojiri, and M. Motokawa Edts. Application of Submillimeter Wave Electron Spin Resonance for Novel Magnetic Systems, J. Phys. Soc. Jpn. **72** Suppl. B (2003).
[6] S. A. Zvyagin, M. Ozerov, E. Čižmár, D. Kamenskyi, S. Zherlitsyn, T. Herrmannsdörfer, J. Wosnitza, R. Wünsch and W. Seidel Rev. Sci. Instrum. **80**, 073102-1-7 (2009).
[7] E. J. Reijerse, Appl. Magn. Reson. **37**, 795 (2010).
[8] B. Cage and S. Russek, Rev. Sci. Instrum. **75**, 4401 (2004).
[9] T. Sakurai, R. Goto, N. Takahashi, S. Okubo, and H. Ohta, J. Phys.: Conf. Ser. **334**, 012058-1-4 (2011).
[10] W. M. Walsh, Jr. and N. Bloembergan, Phys. Rev. **107**, 904 (1957).
[11] I. P. Kaminow and R. V. Jones, Phys. Rev. **123**, 1122 (1961).
[12] J. Stankowski, A. Gałęzewski, M. Krupski, S. Waplak, and H. Gierszal, Rev. Sci. Instrum. **47**, 128 (1976).
[13] J. D. Barnett, S. D. Tyagi, and H. M. Nelson, Rev. Sci. Instrum. **49**, 348 (1978).
[14] M. Krupski, Rev. Sci. Instrum. **67**, 2894 (1996).
[15] N. Sakai and J. H. Pifer, Rev. Sci. Instrum. **56**, 726 (1985).
[16] S. E. Bromberg and I. Y. Chan, Rev. Sci. Instrum. **63**, 3670 (1992).
[17] S. Garaj, T. Kambe, L. Forró, A. Sienkiewicz, M. Fujiwara, and K. Oshima, Phys. Rev. B **68**, 144430-1-7 (2003).
[18] A. Sienkiewicz, B. Vileno, S. Garaj, M. Jaworski, and L. Forró, J. Magn. Reson. **177**, 261 (2005).
[19] S. Haravifard, A. Banerjee, J. C. Lang, G. Srajer, D. M. Silevitch, B. D. Gaulin, H. A. Dabkowska, and T. F. Rosenbaum, Proc. Natl. Acad. Sci. **109**, 2286 (2012).
[20] T. Sakurai, A. Taketani, S. Kimura, M. Yoshida, S. Okubo, H. Ohta, H. Tanaka, and Y. Uwatoko, AIP Conf. Proc. **850**, 1057 (2006).
[21] T. Sakurai, M. Tomoo, S. Okubo, H. Ohta, K. Kudo, and Y. Koike, J. Phys.: Conf. Ser. **150**, 042171-1-4 (2009).
[22] T. Sakurai, T. Horie, M. Tomoo, K. Kondo, N. Matsumi, S. Okubo, H. Ohta, Y. Uwatoko, K. Kudo, Y. Koike, and H. Tanaka, J. Phys.: Conf. Ser. **215**, 012184-1-4 (2010).
[23] Y. Uwatoko, T. Hotta, E. Matsuoka, H. Mori, T. Ohki, J. L. Sarrao, J. D. Thompson, N. Mōri, G. Oomi, Rev. High Pressure Sci. Technol. **7**, 1508 (1998).
[24] T. Sakurai, A. Taketani, T. Tomita, S. Okubo, H. Ohta, and Y. Uwatoko, Rev. Sci. Instrum. **78**, 065107-1-6 (2007).
[25] T. Sakurai, K. Fujimoto, R. Goto, S. Okubo, H. Ohta, and Y. Uwatoko, J. Magn. Reson. **223**, 41 (2012).